Magnetism of Fe/V and Fe/Co multilayers

2003 J. Phys.: Condens. Matter 15 S599

(http://iopscience.iop.org/0953-8984/15/5/313)

INSTITUTE OF PHYSICS PUBLISHING JOURNAL OF PHYSICS: CONDENSED MATTER

J. Phys.: Condens. Matter **15** (2003) S599–S615 PII: S0953-8984(03)55334-6

Magnetism of Fe/V and Fe/Co multilayers

O Eriksson[1], L Bergqvist[1], E Holmström[1], A Bergman[1], O LeBacq[2], S Frota-Pessoa[3], B Hjörvarsson[1] and L Nordström[1]

[1] Department of Physics, Uppsala University, Box 530 Uppsala, Sweden
[2] Laboratoire de Physique et Modélisation des Milieux Condensés, Maison des Magistères, CNRS, BP 166, 38042 Grenoble, France
[3] Instituto de Fisica, Universidade de Sao Paulo, CP 66318, 05315-970, Sao Paulo, SP, Brazil

Received 29 October 2002
Published 27 January 2003
Online at stacks.iop.org/JPhysCM/15/S599

Abstract

We discuss in this paper the magnetic and structural parameters of Fe/V and Fe/Co multilayers. The electronic structure, magnetic moments (spin and orbital) and Curie temperatures as well as the magneto-crystalline anisotropy are calculated using first principles theory. Although theory is fairly successful in reproducing the experimental data we argue that the observed difference between theory and experiment most likely is due to lattice imperfections and that the interface between e.g. Fe and V is not perfectly sharp. We also present a model, based on the theory of elasticity, for analysing the structural properties of multilayers.

(Some figures in this article are in colour only in the electronic version)

1. Introduction

The magnetic and structural properties of Fe/V multilayers have been under focus recently, both theoretically and experimentally. This is largely motivated by the fact that these multilayers are ideal model systems to study magnetism in reduced dimensionality, where one can monitor a transition from three dimensional to quasi-two dimensional, by modifying the thickness of the Fe and V layers. Hence there have been several experimental studies of these multilayers measuring the magnetic moments [1–3], the structural properties [4], the in-plane [5] and out-of-plane magneto-crystalline anisotropy [6] and the interlayer exchange coupling. As a result of these studies it has been established that the Fe atoms carry a reduced magnetic moment at the interface with the V atoms and that the V atoms also carry a magnetic moment coupled antiparallel to the Fe moment. The size of the Fe interface moment is reported to be 1.2 μ_B and that of V is reported to be 0.5 μ_B. Theoretical calculations are rather successful in

reproducing this behaviour; the anti-ferromagnetic coupling between Fe and V is reproduced, the reduced Fe moment at the interface and the size of the V moment are at least with some success reproduced by theory. Although theory has been rather successful in reproducing the measured magnetic properties of these multilayers there are marked differences that will be addressed in this paper, and we argue that this disagreement is due to structural imperfections at the Fe/V interface.

It was recently observed that since the V atoms absorb hydrogen one has the possibility to control the structural properties (lattice parameters) of the V layers, at least to some extent. More importantly it has been found that the absorption of H in the V layers offers a way to control the interlayer exchange coupling [7]. Hence the coupling between Fe layers, which e.g. in Fe_3V_{12} and Fe_3V_{14} is antiferromagnetic, becomes ferromagnetic when small amounts of hydrogen are allowed to enter the films. In addition it has been observed that when Fe/V multilayers are exposed to hydrogen gas it is only the V layers that actually absorb H and that H is not found for 1–2 V layers close to the interface with Fe.

Fe/Co has also been the subject of considerable interest, not least due to the potential in using these alloys as materials in write-heads in magnetic recording devices [8]. Bulk alloys have been investigated in some detail, and the magnetic moments are found to follow the Slater–Pauling curve, with an initial increase in average moment with increasing Co concentration. The maximum average magnetic moment is reached for a concentration of $\sim$25% Co and the average spin moment for this alloy concentration is $\sim$2.3 μ_B/atom [9]. Together with an orbital moment of $\sim$0.1 μ_B/atom for this concentration [9] a maximum total moment of $\sim$2.4 μ_B/atom is obtained for bulk bcc FeCo alloys. It should be noted that higher values of the total moment of FeCo alloys have been quoted, e.g. reference [10] gives an average moment of $\sim$2.5 μ_B/atom. A few magnetization studies were also reported on films and multilayers, and it was concluded that for films with low Co concentration the multilayers give average moments lower than that of the bulk alloy, whereas for films with high Co concentration the opposite situation is found [11]. Structural properties of Fe/Co multilayers were also reported [12, 13] and in particular short range ordering of the Fe and Co atoms was discussed, something which might also have implications for the magnetic properties.

First principles theory reproduces the behaviour of the bulk moments of FeCo alloys, in particular the lower moments that have been quoted [9]. An early model calculation, based on the virtual crystal approximation, reproduced both the spin and orbital moments of bcc FeCo [14], whereas more accurate calculations based on the coherent potential approximation (CPA) gave similar results for the spin moments [15–18] (the orbital moment was not evaluated). In the case of thin FeCo alloy films on Cu, theory showed that the moments of both Fe and Co were enhanced substantially. A magnetization profile was also reported for Fe/Co multilayers [19], using first principles calculations, and among the more conspicuous findings is the observed enhanced Fe moment at the Fe/Co interface, where the Fe atom was shown to carry a moment as high as 2.6 μ_B/atom. The Co atoms were found to have similar moments in the bulk of the film and at the interface, typically being of the order of 1.75 μ_B/atom.

We review here some of the pertinent experimental and theoretical results of the Fe/V and Fe/Co multilayers and show, using first principles theoretical calculations, that the interface between the Fe and V layers of the Fe/V multilayers must be less sharp than thought originally. By means of a theoretical model that incorporates both interchange of Fe and V atoms across the interface, resulting in an alloy phase at the interface, and terrace-like structures at the Fe/V interface, we reproduce the magnetic moments and the critical temperatures as well as the interlayer exchange coupling.

2. Theory

The calculational method used in part of this work is the full-potential linearized muffin-tin orbital (FP–LMTO) method [20]. This method makes no approximation to the shape of the potential or charge density and is all electron and fully relativistic. For the calculations of orbital moments and magnetic anisotropy energy (MAE), relativity is crucial. The calculations of the MAE were made using the force theorem, which has been tested for these systems to be accurate within 10% [21].

In the calculations of the interface roughness effects we used the Korringa, Kohn and Rostocker (KKR) [22] method within the atomic-sphere approximation (ASA) together with the local spin density approximation as parametrized in [23]. To carry out the partly alloyed multilayer calculations, we used the CPA [24].

The magnetic properties and electronic structure of the Fe/Co multilayers have also been calculated with a real space LMTO–ASA method [25]. This RS–LMTO–ASA scheme is similar to the standard k-space LMTO–ASA scheme, but uses the recursion method [26] to solve the eigenvalue problem, formulated within the LMTO–ASA formalism, to calculate the local density of states (LDOS). The LDOS is obtained from a continued fraction of the calculated recursion coefficients using a Beer–Pettifor terminator. In this work, we used fully relativistic calculations, so that both spin and orbital moments were obtained. The cut-off factor for the recursion used here was 24 and the perfect interfaces were calculated for clusters of around 10 000 atoms. With this real space technique, local perturbations such as impurities [27] can easily be treated without using large supercells. The method has been compared with traditional k-space calculations [25] and with KKR–GF methods [27] and shows good agreement. In this work the RS–LMTO–ASA method was used only in the study of Fe/Co multilayers and in the calculations we used the experimental lattice constants of these films [28].

3. Fe/V multilayers

3.1. Spin and orbital moments of ideal structures

In this section we discuss the spin and orbital moments of three multilayer systems, Fe_2V_6, Fe_3V_5 and Fe_4V_4. The calculations of magnetic properties were made assuming the experimental lattice parameters but with a perfect crystal structure, as illustrated in figure 1. The numerical values of the calculated layer resolved spin and orbital magnetic moments are tabulated in table 1. Our numerical values of Fe_3V_5 can be compared to the LCAO and LMTO–ASA calculations of Moser *et al* [29] for the (001) $(Fe_3V_3)_\infty$ multilayers, who found 1.6 μ_B for Fe at the interface, 2.8 μ_B for the central Fe layer and -0.5 μ_B for the interface V layer, close to our corresponding values, 1.77, 2.70 and -0.40 μ_B, calculated inside the muffin-tin spheres. These results are similar to those obtained by the first-principles LMTO calculation of Süss *et al* [30]. The contribution from the interstitial region remains small and quite independent of the number of Fe layers. The presently calculated value of the total magnetic moment of the Fe_4V_4 multilayers, namely 7.34 μ_B, is only in rough agreement with the recent experiments of Farle *et al* [6], quoting a value of 5.5 μ_B. The discrepancies on the individual site projected magnetic moments are even larger, partly due to the assumption of the authors of [6] fixing the magnetic moment of the Fe(I $-$ 1) atoms to the bulk Fe value (2.2 μ_B) and the value of the V(I) atoms at -0.35 μ_B. Using these assumptions, the magnetic moment of the Fe(I) atoms at the interface has been experimentally estimated to be 1.55 μ_B. Our calculated values are $\mu_{\mathrm{Fe(I-1)}} = 2.52$ μ_B, $\mu_{\mathrm{Fe(I)}} = 1.74$ μ_B and $\mu_{\mathrm{V(I)}} = -0.45$ μ_B.

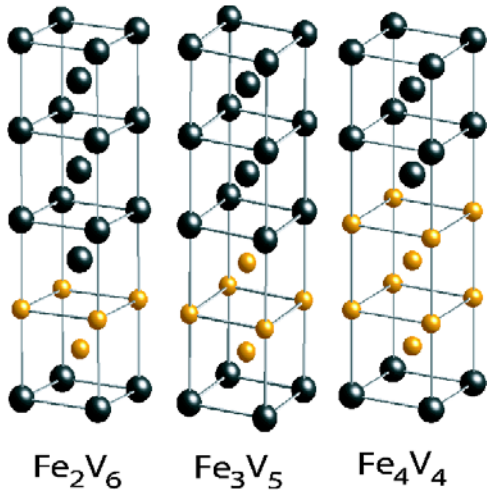

Figure 1. Geometry of the three supercells. The Fe atoms have light colouration and the V atoms dark colouration.

Table 1. Calculated site-projected spin (μ_s) and orbital (μ_ℓ) moments (in μ_B), including the spin–orbit coupling as well as the orbital polarization, inside the MT sphere for the different layers of the Fe_2V_6, Fe_3V_5 and Fe_4V_4 multilayers.

	Fe_2V_6			Fe_3V_5			Fe_4V_4		
	μ_s	μ_ℓ	μ_ℓ/μ_s	μ_s	μ_ℓ	μ_ℓ/μ_s	μ_s	μ_ℓ	μ_ℓ/μ_s
Fe(I-1)	—	—	—	2.70	0.043	0.016	2.52	0.092	0.037
Fe(I)	1.87	0.058	0.031	1.77	0.060	0.034	1.74	0.069	0.040
V(I)	−0.45	0.019	−0.042	−0.40	0.012	−0.030	−0.45	0.020	−0.044
V(I-1)	−0.06	0.004	−0.066	−0.04	0.002	−0.050	−0.01	0.004	−0.400
V(I-2)	−0.04	0.001	−0.025	0.08	0.003	0.038	—	—	—
Interstitial	−0.26			−0.26			−0.28		

The calculated results (table 1) for Fe_2V_6 may also be compared to experiment and previous theory. Anisimov *et al* [31], using the LMTO–ASA method that neglects lattice relaxation, brackets the magnetic moment of the Fe(I) atoms between 1.62 and 2.1 μ_B and that of the V(I) atoms between -0.45 and -0.67 μ_B, provided that the lattice constant is chosen to be the experimental lattice constant of Fe (lower limit), or of V (upper limit). The results presented in table 1 are in good agreement with the data of [31]. However, as done for Fe_4V_4, assuming that the magnetic moment of the interface V atoms are fixed to -0.67 μ_B, Farle *et al* [6] deduced experimental values of 1.14 μ_B for $\mu_{Fe(I)}$ for the Fe_2V_5 multilayer, which appears strongly underestimated with respect to our present calculations (1.87 μ_B) and the theoretical results of Anisimov *et al* [31]. The orbital moments, also listed in table 1, are rather small, which is typical for transition metals, and cannot explain the disagreement between theoretical and experimental moments. A comparison between experimental [6] and theoretical orbital moments show that they agree somewhat better than the spin moments. The overall picture of the spin and orbital moments presented in this section hence show that, where a comparison can be made, there is a distinct disagreement between theory and experiment, something we will return to below.

3.2. Out-of-plane magnetic anisotropy

We turn next to the magneto-crystalline anisotropy of the Fe_2V_6 and Fe_4V_4 multilayers. The direction of the easy axis of magnetization, as well as the magnetic hardness, i.e., how difficult it is to change the magnetization direction, are of fundamental importance for the functionality of these materials. Both these characteristics can be described through the magnetic anisotropy energy (MAE), which has the following definition: the total energy of a magnetic material depends on the direction of magnetization. The energy difference for different directions of magnetization with respect to a reference direction (in this work the (001) direction) is the MAE. Note that here we are only concerned with the contribution that is due to relativistic effects as manifested through the spin–orbit coupling. The total easy axis of magnetization for a macroscopic body with finite extent (i.e., it has shape) depends also on the shape anisotropy. The latter can be large for, e.g., thin films, but in the experimental data that we compare to, the shape contribution has been subtracted.

The calculated MAE of Fe_4V_4 (-11.5 μeV/atom) is of the same order of magnitude as the experimental value (-5 μeV/atom) [6]. The theoretical value deviates by a factor of two from experiment. As regards the Fe_2V_6 multilayers, the MAE is found to be 2.2 μeV/atom. The calculated value is in excellent agreement with the experimental value of the corresponding multilayer, namely 2.0 μeV/atom, obtained by Anisimov *et al* [31] with angular-dependent ferromagnetic resonance (FMR) measurements. For both these multilayers the calculated easy axis, i.e. [001] and [100] for Fe_2V_6 and Fe_4V_4 respectively, agrees with the experiments.

3.3. Critical temperatures

For the calculation of critical temperatures we used a combination of first principles calculations and Monte Carlo simulations which will be described below. First, we used a TB–LMTO–ASA method to calculate a number of non-collinear magnetic configurations in Fe/V multilayers. The implementation of non-collinearity follows the scheme presented by Uhl *et al* [32] and by Kubler [33]. We employed the local density approximation and we have also included the so called combined correction terms to the Hamiltonian as described by Skriver [34]. The magnetic configurations considered in this study are incommensurate spin spiral structures and they are defined by giving the Cartesian coordinates of the magnetization vector $\vec{m}_{n\nu}$ as [35]

$$\vec{m}_{n\nu} = m_\nu[\cos(\vec{q}\cdot\vec{R}_n + \phi_\nu)\sin\theta_\nu, \sin(\vec{q}\cdot\vec{R}_n + \phi_\nu)\sin\theta_\nu, \cos\theta_\nu]. \tag{1}$$

Here m_ν is the magnetic moment at site $\vec{r}_\nu$, n labels the atom at $\vec{R}_n$ and $(\vec{q}\cdot\vec{R}_n + \phi_\nu)$ and $\sin\theta_\nu$ are polar angles (Euler angles). By varying the Euler angles for different atoms one can tune the response of the spin spiral which will be important as we will see later. For instance, an atom will not contribute to spin spiral energies if one chooses $\theta_\nu = 0$ for that particular atom.

The spin spiral energies are mapped through a least squares fit to a classical Heisenberg model including biquadratic exchange interactions. The Hamiltonian has the form

$$H = -\tfrac{1}{2}\sum_{i\neq j} J_{ij}\vec{e}_i\cdot\vec{e}_j - \tfrac{1}{2}\sum_{i\neq j} K_{ij}(\vec{e}_i\cdot\vec{e}_j)^2, \tag{2}$$

where J_{ij} and K_{ij} are exchange parameters.

In order to obtain thermodynamic properties such as the critical temperature one needs to solve a statistical mechanics problem. The most common way to solve this problem is to use mean field theory (MFT) in which the expression for critical temperature reads (with bilinear interactions only)

$$k_B T^{MFT} = \tfrac{1}{3}\sum_j J_{0j}. \tag{3}$$

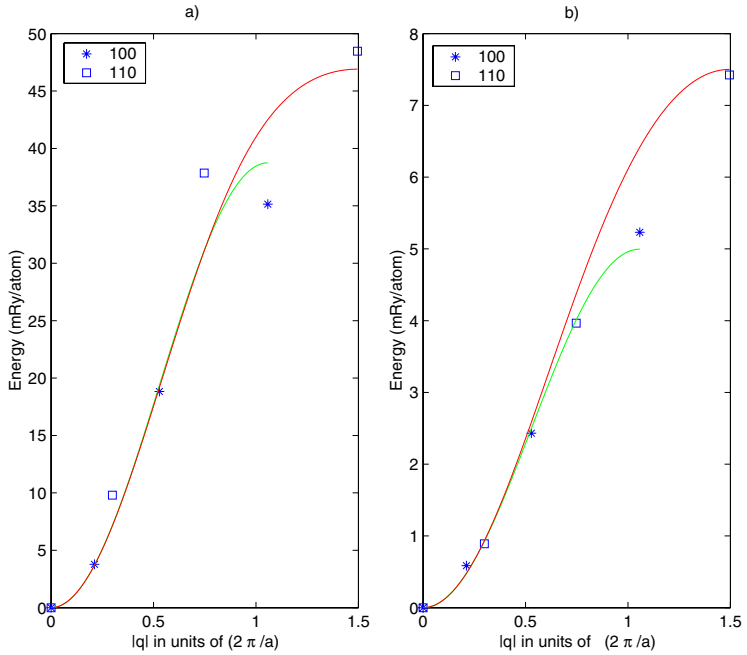

Figure 2. Calculated spin wave energies for Fe_3V_7 along the 100 and 110 directions. The symbols represent calculated values and the lines the fitted values (equation (2)). In (a) θ is set to 90° for all layers and in (b) it is set to 90° for the central atoms and 0° for the interface atoms.

However, it is well known that MFT is valid only in higher dimensions. Since we are dealing with low dimensionality systems, MFT clearly is not the appropriate choice to use. We have instead used Monte Carlo simulations to solve the statistical mechanics problem. Monte Carlo is a step beyond MFT since it includes fluctuations which are absent in MFT, that are important especially for low dimensionality systems.

We use the standard single flip Metropolis algorithm as described in great detail in [36]. To determine critical temperature T_c we have used the 'cumulant crossing method'. We then calculate the reduced fourth order cumulant of the order parameter (magnetization) U_L, defined as

$$U_L = 1 - \frac{\langle M^4 \rangle}{3\langle M^2 \rangle^2} \tag{4}$$

for different lattice sizes. The curves of U_L will have a common intersection at a fixed point U^*, which will be the critical point. Hence, we obtain a value of T_c from the intersection point of U_L for different lattice sizes. A full account of these calculations will be given elsewhere [37].

We have calculated T_c for Fe_2V_6 and Fe_3V_7 multilayers. Due to the similarity in technical details of the two systems, we will give the details only for the calculation of Fe_3V_7. We have in this study considered the case of perfect interfaces with no intermixing between the Fe and V interface layers. We set up a multilayer geometry and calculated the energy $E(\vec{q})$ for a number of spin spirals using the force theorem. The results are shown in figure 2. We choose spirals in the [100] and [110] directions. We then fit the spiral energies to our model Hamiltonian (equation (2)) to obtain exchange interactions. In order to obtain all exchange interactions we first set the Euler angle $\theta_v = \pi/2$ for all the Fe layers as shown in figure 2(a). All three Fe layers will then contribute to the spin spiral energies. In the second set of calculations, we

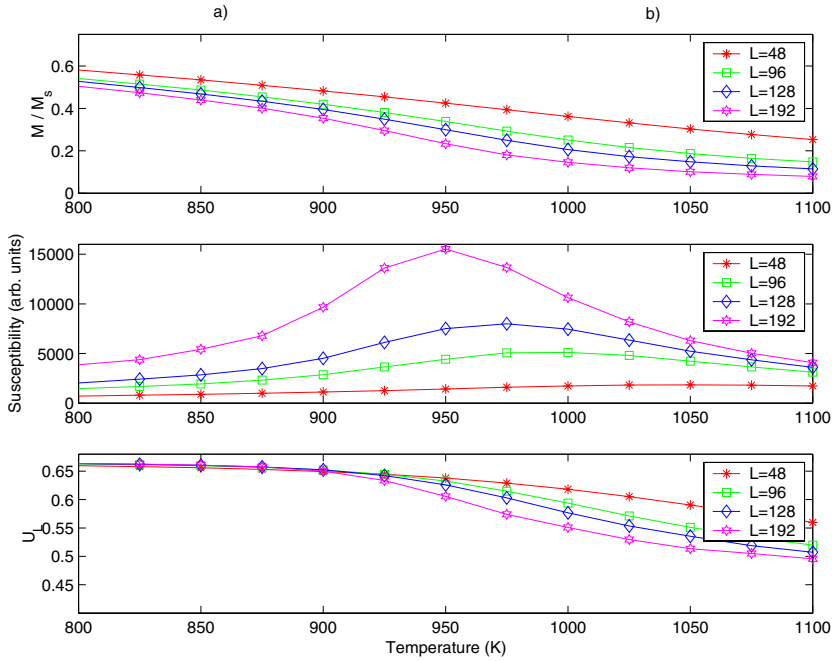

Figure 3. Monte Carlo simulation of the critical temperature of Fe_3V_7. The top curve represents the magnetization, the middle curve the susceptibility and the lower curve the fourth order cumulant. Simulations for different sizes of the cell are given with the length of the simulation cell being $L = 48$, 96, 128 and 192 lattice spacings.

set the Euler angle $\theta_\nu = \pi/2$ *only* in the central layer and $\theta_\nu = 0$ in the two interface layers as shown in figure 2(b). Then the only contribution to the spin spiral energies will be from the central layer. In this way one can extract information about exchange interactions in each layer and also between the different Fe layers in Fe_3V_7

Once all exchange interactions are obtained within and between all atomic layers, we perform a number of Monte Carlo simulations to extract T_c. We use a simulation box of dimension $L \times L \times D$, where D is the thickness and L has been varied from 48 to 192. The interlayer exchange coupling between the Fe layers was set to a typical value of 1 meV, but the value of T_c is weakly dependent on this coupling. The total number of MCSs/spin was around 50 000, where the averages of the thermodynamic observable were measured in the last 15 000 steps. Results are shown in figure 3. The calculated critical temperature extracted from the cumulant is 910 K, compared to the experimental value of around 400 K [1–3]. We repeated the same kind of calculation for Fe_2V_6 and obtained a critical temperature of 850 K which is much higher than the experimental value of around 200 K [1–3]. The theoretical method used here reproduces the critical temperatures of transition metals in the bulk [37], and judging from the poor agreement between experiment and theory for these multilayers we conclude that it is likely that, just as concerns the magnetic moments, the interface between the Fe and V layers is not perfectly atomically sharp.

3.4. The effect of interface roughness

From the findings presented above, where the experimental magnetic moments, MAE and critical temperatures are reproduced to some extent by theory, but where differences are clearly

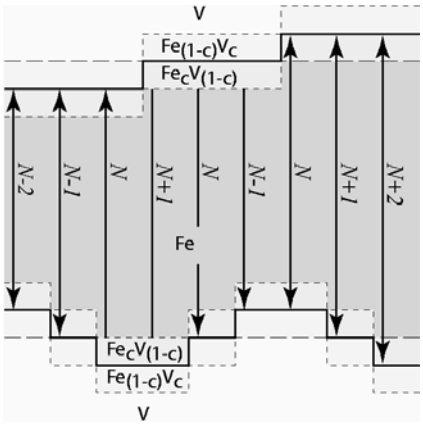

Figure 4. Model of the interface between the Fe and V layers. The white area denotes the V layers, the dark grey area the Fe layers and the light grey area the alloyed layers.

discernible, we come to the conclusion that the interface between the Fe and V layers is not atomically sharp. A very good indicator of the interface quality in Fe/V multilayers is the total magnetization of the sample divided by the number of Fe atoms. The reason for this is that the magnetic moment of the Fe atom is very sensitive to the number of nearest neighbouring V atoms [38]. Having made this observation, we construct a model of interface imperfections that is an extension of the two models that were suggested by Kudrnovsky *et al* [39].

The first effect, thickness variation, is modelled by flat terraces of monolayer height at the interfaces fluctuating randomly in both directions around an ideal interface. The ratio between the area covered by one type of step and the total area is denoted γ and the two types of imperfection, i.e. depletions and protrusions, are assumed to be present with the same probability.

The other effect, interface interdiffusion, is calculated directly by letting the atomic layers at each interface mix and form a random substitutional alloy. This means that each atomically sharp Fe/V interface is in fact an interface of the type Fe/Fe$_c V_{(1-c)}$/Fe$_{(1-c)}$V$_c$/V. When we tried these two models for interface imperfections we found that employing either of them separately did not reproduce the experimentally measured values of the magnetic moment. We then investigated if a combination of the effects could account for the discrepancy between the theoretical and experimental values. An illustration of the structural profile of the thickness variation together with the interface interdiffusion is shown in figure 4. Each Fe slab in a Fe/V superlattice has two interfaces and each has a probability of deviating from its ideal position by the probability constant γ. At the same time we let each interface intermix in the two atomic layers closest to the interface. In practice, we calculate the superlattices without the steps but with interdiffused interfaces to get a total magnetic moment for each concentration: M_c(Fe$_m$V$_n$) where $\{c\} = (0; 0.1; 0.2; 0.3; 0.4; 0.5)$. Then, in order to include the effects from the thickness variation, we calculate the probabilities of the possible thicknesses that are allowed by the assumptions of the interfaces, i.e. $N \pm 2$, $N \pm 1$ and N. In total we then have to perform one calculation for each concentration (6) and each thickness (5) i.e. $5 \times 6 = 30$ calculations for each superlattice Fe$_m$V$_n$. The total moment is then dependent on the parameters γ and c and is here given in a matrix form,

$$M_c^{\gamma}(\mathrm{Fe}_m\mathrm{V}_n) = \sum_{i=-2}^{2} M_c(\mathrm{Fe}_{n-i}\mathrm{V}_{m+i})\,P(N+i) \tag{5}$$

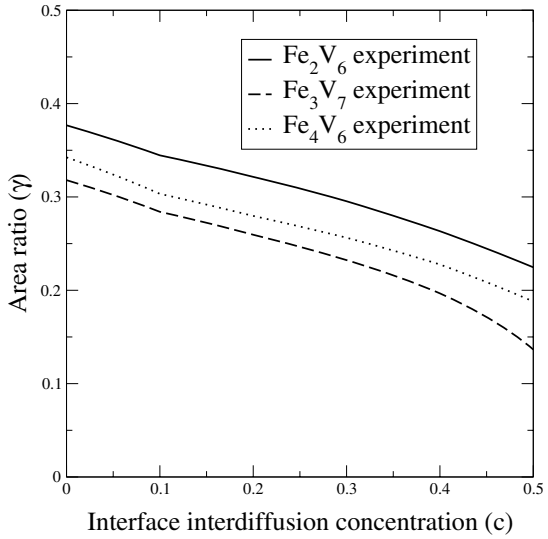

Figure 5. Magnetic moment in the concentration (c)–roughness (γ) phase space (for details see text), for three different multilayers.

where the slab-thickness probability function P is defined as

$$P(N-2) = \gamma^2$$
$$P(N-1) = 2\gamma(1-2\gamma)$$
$$P(N) = 2\gamma^2 + (1-2\gamma)^2$$
$$P(N+1) = 2\gamma(1-2\gamma)$$
$$P(N+2) = \gamma^2.$$

The matrix $M_c^{\gamma}(\mathrm{Fe}_m\mathrm{V}_n)$ may then contain a line with the experimental moment that can be drawn in the phase space $\{c, \gamma\}$. An interesting comparison can be made by calculating the same matrix for another superlattice and investigating whether the new experimental line falls in the same area of the phase space. In figure 5 we have plotted experimental lines for the superlattices Fe_2V_6, Fe_3V_7 and Fe_4V_6 in the phase space $\{c, \gamma\}$. The experimental lines were taken from the linear fit to the values given in [31], and we observe that the three experimental lines cut through the same region in the $\{c, \gamma\}$ phase space. This is a good test of the validity of our model since the three multilayers are expected to grow with similar quality.

3.5. A growth model for Fe/V

The analysis presented above suggests that there is considerable intermixing between the Fe and V atoms at the interface, but despite this fact it is interesting to analyse the measured in-plane and out-of-plane lattice constants for these multilayers assuming a model based on the classical theory of elasticity and ideal atomically sharp interfaces. In the limit of thick Fe or V layers the effect of interface roughness becomes negligible and the model we propose below should be viewed as applicable in this regime. Experimental values of the in-plane and out-of-plane lattice constants have been measured for Fe (20 Å)/V (x Å) multilayers [5], where Fe (20 Å) indicates that the Fe thickness was kept fixed at 20 Å whereas the V thickness (x Å) was varied. In our elasticity model there are two main contributions to the total energy of each

layer (Fe and V) of the multilayer. To accomplish the common in-plane lattice parameter, the Fe and V layers are allowed to distort the structural properties (becoming tetragonal) as well as to modify the volume, so that the in-plane lattice parameters coincide. The balance between volume change and degree of tetragonal distortion is entirely given by the elastic constants of Fe and V, in a way that will be described below. Let us first evaluate the energy contribution from the tetragonal distortion, that is written as [40]

$$E_s = E_0 + 6c'\delta^2 V, \tag{6}$$

where c' is related to the elastic constants c_{11} and c_{12} through $c' = 1/2(c_{11} - c_{12})$, and δ is defined through the c/a ratio as

$$\frac{c}{a} = \frac{a_\perp}{a_\parallel} = \frac{1}{(1+\delta)^3}. \tag{7}$$

The energy associated with a change in volume can be expressed as

$$E_v = E_0 + \frac{\partial E_v}{\partial V}\Delta V + \frac{1}{2}\frac{\partial^2 E_v}{\partial V^2}(\Delta V)^2 + \cdots, \tag{8}$$

where the first term is the energy corresponding to the equilibrium volume, the second term is zero since the distortion is made from an equilibrium configuration and the third term is related to the bulk modulus, B, as

$$B = V\frac{\partial^2 E_v}{\partial V^2}. \tag{9}$$

The change in volume is given by $\Delta V = 1/2(a_\perp a_\parallel^2 - a_0^3)$, where $a_\parallel$ and $a_\perp$ are the in- and out-of-plane lattice parameters of the tetragonally strained film and a_0 is the lattice parameter of the unstrained cubic crystal. Note that the factor $1/2$ comes from the fact that there are two atoms/conventional unit cell in the bcc structure. B is the bulk modulus, which is defined through $B = (c_{11} + 2c_{12})/3$. As an approximation, the values used for c' and B are here taken as the bulk ones, although for a multilayer consisting of thin layers they are expected to deviate, and could be calculated. The two contributions are now added,

$$E_{\mathrm{tot}} = E_0 + 6c'\left[\left(\frac{a_\parallel}{a_\perp}\right)^{\frac{1}{3}} - 1\right]^2 a_0^3 + \frac{B}{2a_0^3}(a_\perp a_\parallel^2 - a_0^3)^2. \tag{10}$$

For a superlattice consisting of N_{Fe} layers of Fe and N_{V} layers of V, the appropriate total energy is

$$E_{\mathrm{tot}} = N_{\mathrm{Fe}}E_{\mathrm{Fe}} + N_{\mathrm{V}}E_{\mathrm{V}}. \tag{11}$$

The equilibrium configuration is then found from minimizing this energy with respect to the lattice parameters, requiring that $\partial E_{\mathrm{tot}}/\partial a_\parallel = 0$, $\partial E_{\mathrm{tot}}/\partial a_\perp^{\mathrm{Fe}} = 0$ and $\partial E_{\mathrm{tot}}/\partial a_\perp^{\mathrm{V}} = 0$.

The in-plane lattice parameter deduced from the XRD and the theoretical calculation is shown in figure 6 and we observe that the agreement between theory and experiment is decent. The theoretical model overestimates the lattice constants by a small amount and one may also observe that the slopes of the theoretical and experimental curves are somewhat different. For comparison we also show the lattice constants of a bcc FeV alloy, calculated from Vegard's law. One may note that the models based on elasticity and Vegard's law have roughly the same slope and give rather similar lattice constants, whereas the experimental curves have a slightly different form. Unfortunately, no experimental data exist for the out-of-plane lattice constants of Fe and V; only the average is obtained experimentally. In the XRD experiment the weighted average of the out-of-plane lattice parameter is measured, i.e.

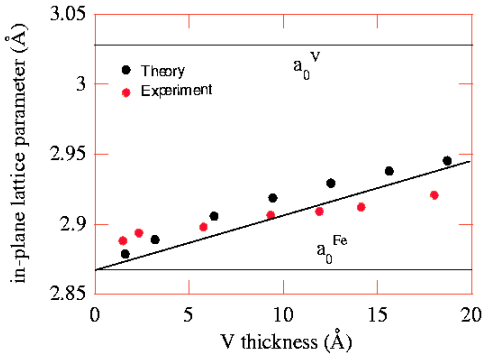

Figure 6. In-plane lattice spacing for the Fe/V multilayer as a function of V thickness. The experimental data are given as grey circles, the data from the elasticity model by black circles and the lattice spacings using Vegard's law for a bulk FeV alloy are given by the slanted line.

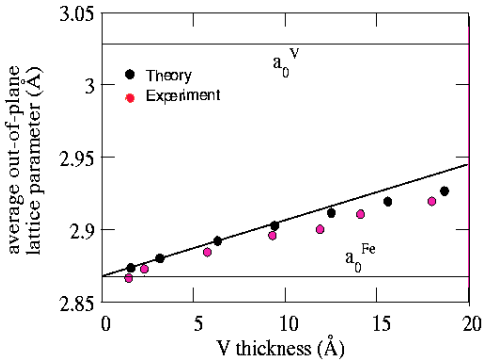

Figure 7. Out-of-plane lattice spacing for the Fe/V multilayer as a function of V thickness. The experimental data are given as grey circles, the data from the elasticity model by black circles and the lattice spacings using Vegard's law for a bulk FeV alloy are given by the slanted line.

$$\langle a_\perp \rangle = \frac{N_{\mathrm{Fe}} a_\perp^{\mathrm{Fe}} + N_{\mathrm{V}} a_\perp^{\mathrm{V}}}{N_{\mathrm{Fe}} + N_{\mathrm{V}}}. \tag{12}$$

In figure 7, both the measured and theoretical average out-of-plane lattice parameters are plotted. In this figure the lattice constant of a bulk alloy, obtained from Vegard's law, is given. For the average out-of-plane lattice constant this approximation gives a less accurate description of the structural properties, whereas the elastic model discussed above reproduces experiment more accurately. One may of course expect larger deviations from Vegard's law in multilayers that are built up from materials with drastically different elastic constants.

One more important fact from figures 6 and 7 can be observed, namely that the experimental curves do not approach the experimental Fe lattice constant in the limit of vanishing V thickness. For the out-of-plane lattice constant experiments extrapolate to a somewhat smaller value and for the in-plane constant experiments extrapolate to a larger value. The volume of the 'Fe' multilayer given in the limit of vanishing V thickness is a few per cent larger that the volume of bulk bcc Fe. This suggests again lattice imperfections at the interface, so that in the limit of vanishing V thickness one does not extrapolate to the lattice constant of pure bcc Fe but to the lattice constant of an FeV alloy or a bcc Fe film with vacancies or interstitial impurities.

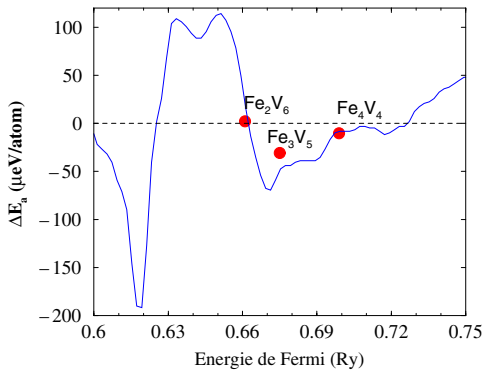

Figure 8. MAE of Fe–V multilayers as a function of the Fermi energy. The self-consistent calculation of the MAE (circles) is added for comparison, at three band fillings corresponding to Fe_2V_6, Fe_3V_5 and Fe_4V_4. For values of the MAE larger than zero the 001 axis is the easy axis, and for smaller values of the MAE the easy axis is in plane.

3.6. Chemical effects and magnetic anisotropy energy

We have argued that the interfaces between the two elements that constitute the multilayers cannot be expected to be perfect, so that the proportions between the two elements also vary slightly from one layer to another. One way to investigate the sensitivity of the MAE with respect to the relative proportions of the elements constituting the multilayers consists in studying the variation of the MAE of the Fe–V systems with respect to the d-band filling. For this purpose, we proposed a band-filling model [21] aiming at expressing the MAE of the Fe–V system as the Fermi energy of our compounds is varied, i.e. as the d band of Fe atoms is increasingly filled. To obtain this dependence of the MAE with respect to the Fermi energy, we have integrated the densities of states of the Fe_4V_4 multilayer, $D^{\sigma}(\epsilon)$ with $\sigma =$ [001] and [100] (corresponding to 52 valence electrons in the unit cell) in an energy range starting from 0.45 Ryd (from which the [001] and [100] DOSs start to be nondegenerate) to a Fermi energy that we allow to vary by a small amount (using the rigid band approximation). We obtained the following final expression for the MAE:

$$E_a(E_F) = \int_{-\infty}^{E_F} \delta N(\epsilon)\, \mathrm{d}\epsilon, \tag{13}$$

where E_F is the Fermi energy, and $\delta N(\epsilon) = N^{[100]}(\epsilon) - N^{[001]}(\epsilon)$ is the difference of the integrated DOS, evaluated at the energy ϵ. For selected values of the Fermi energy, corresponding to 49 and 46 electrons, we expect to reproduce the MAE of Fe_3V_5 and Fe_2V_6 which presents these exact band-fillings, respectively. This method allows us to study the effects of band filling, by getting rid of any crystallographic interferences: the DOSs remain the same as the Fermi energy is gradually varied and correspond to a frozen Fe_4V_4 cell (no lattice parameter is changed). Figure 8 displays the so-obtained variation of the out-of-plane MAE of the Fe–V systems with respect to the Fermi energy. The values of the MAE of Fe_4V_4, Fe_3V_5 and Fe_2V_6, obtained by the exact DFT calculations (or using the exact eigenvalues of the respective compounds) are superimposed at their respective Fermi energy.

The results show that, despite noticeable discrepancies attributed to differences between the volume and axial ratio of Fe_3V_5 and Fe_2V_6 and the ones of Fe_4V_4, the sign and the amplitude of the MAE of the three systems agree with the exact calculations, demonstrating that the band-filling effects determine the value of the MAE in these systems to a large extent.

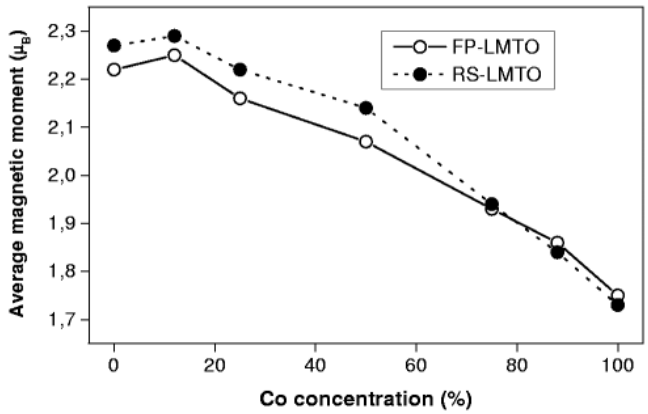

Figure 9. Calculated average spin moments of Fe/Co multilayers using the FP–LMTO method (open circles) and the RS–LMTO–ASA method (black circles). The calculated points are for bcc Fe, Fe_7Co_1, Fe_6Co_2, Fe_4Co_4, Fe_2Co_6, Fe_1Co_7 and Co.

Our results also demonstrate that it should be possible to enhance the MAE of the Fe–V multilayers, while anchoring the magnetization along the [001] spin-direction by tuning the Fermi energy towards lower energies. The substitution of Fe atoms by Mn atoms, reducing the valence of the unit cell, will generate a positive increase of the MAE (providing the coupling between Fe and Mn stays ferromagnetic—see figure 8), re-enforcing the stability of the magnetization along the [001] direction of polarization.

4. Fe/Co multilayers

4.1. Spin and orbital moments

Next we report on the calculated spin and orbital moments of the Fe/Co multilayers. The theoretical work was done with two methods, the full-potential method, that was also used for the calculations of the Fe/V multilayers, and an RS–LMTO–ASA method [25]. We compare in figure 9 the average spin moments from the two methods, for (bcc) Fe/Co multilayers, assuming an ideal interface between the Fe and Co atomic layers. It should be noted that the structure used in the calculations was not ideal bcc, but bct with in-plane and out-of-plane lattice constants taken from experimental data [28]. As can be seen the two methods give very similar values for the spin moments. The real space method typically gives a moment 0.05 μ_B/atom larger than the full potential result. One may also note that figure 9 shows a different trend in the average spin moment, compared to bulk (bcc) FeCo alloys [16], where, as a function of increasing Co concentration, there is initially a sharp upturn in the average moment so that the maximum alloy moment of 2.3 μ_B is found for $\sim$25% Co. For the multilayers the situation is different, the calculated average moment is increasing slowly for low Co concentrations, but changes slope at $\sim$10% Co concentration, to become decreasing with increasing Co concentration.

The lower average moment of the multilayer, compared to bulk, is in agreement with the experimental work of [11] and can be understood from the site projected moments (see below and [15, 16]), that show that the moment of the Fe atom is enhanced (becoming as large as 2.6 μ_B) if the concentration of nearest neighbouring Co atoms is high. Since the Co concentration in the first neighbour shell of the Fe atoms is higher for random bulk alloys compared to that of ideal multilayers (since in this case the Fe and Co atoms are separated in

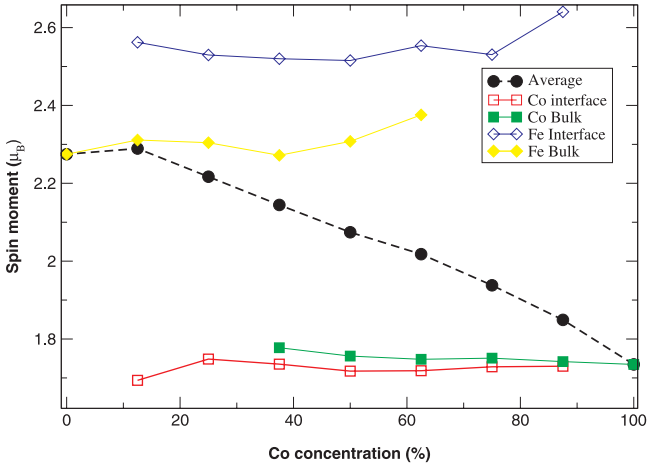

Figure 10. Calculated layer resolved spin moments of Fe/Co multilayers using the the RS–LMTO–ASA method. The calculated points are for bcc Fe, Fe_7Co_1, Fe_6Co_2, Fe_4Co_4, Fe_2Co_6, Fe_1Co_7 and Co.

different atomic layers) it is natural that the average moments of bulk random multilayers is higher.

In figure 10 we display the individual spin moments of the interface and of 'bulk' Fe and Co atoms and in figure 11 we show corresponding values for the orbital moments (obtained from the real space method). The Co spin moments are similar for the interface and for the bulk environment, reflecting the fact that the spin up band of Co is almost completely filled. For Fe this is not the case and consequently any narrowing of bands due to the interface environment will cause a change in the spin moment. As figure 10 shows, the interface moments are larger than the bulk Fe moments, and our calculated values are in agreement with those of Nicklasson *et al* [19]. The orbital moments follow a different trend; here it is the Fe moments that are almost the same for the interface and 'bulk' atoms, whereas the Co moments are lowered for the interface compared to the 'bulk' environment. Summing the spin and orbital moments from the real space method gives a maximum magnetic moment for these films for a Co concentration of ∼10% with a value of ∼2.35 μ_B/atom. The total moment (spin and orbital) from the full potential method is ∼2.30 μ_B/atom for this Co concentration. These values are smaller than the calculated values for bulk bcc FeCo alloys [40] that reproduce the maximum total moment of 2.40 μ_B/atom at a Co concentration of ∼20%.

4.2. Magneto-crystalline anisotropy

In figure 12 we show our calculated in-plane MAE of the bcc Fe/Co multilayers. Note that the calculations reproduce the [100] easy axis for bcc Fe and that there is a transition from [100] to [110] easy axis at a concentration of ∼50% Co. For bulk bcc Fe/Co alloys the easy axis changes from [100] to [110] at a concentration of 40–50% Co [41], i.e. rather close to our calculated values for the multilayers. It is of course natural to expect that there are differences between bulk and thin film data, but one must also consider the very small values of the MAE for these systems, and that theory might make a small error in the exact values of the concentration where the easy axis changes direction. Previously it has been argued that one needs to include corrections to the effective potential in these types of calculation, and the LDA (or GGA) potential has been replaced with the phenomenological LDA + U

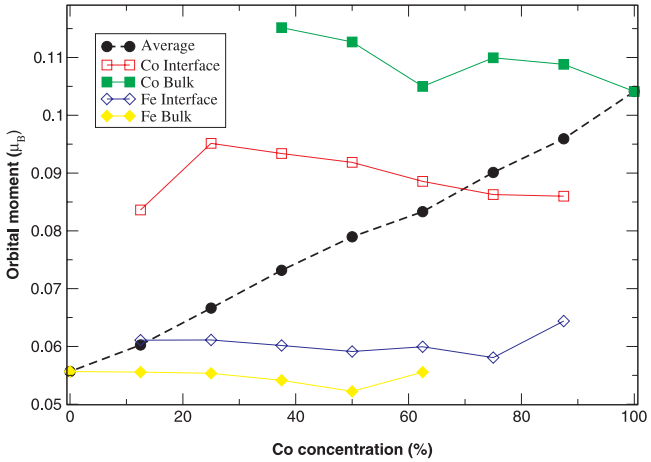

Figure 11. Calculated layer resolved orbital moments of Fe/Co multilayers using the the RS–LMTO–ASA method. The calculated points are for bcc Fe, Fe_7Co_1, Fe_6Co_2, Fe_4Co_4, Fe_2Co_6, Fe_1Co_7 and Co.

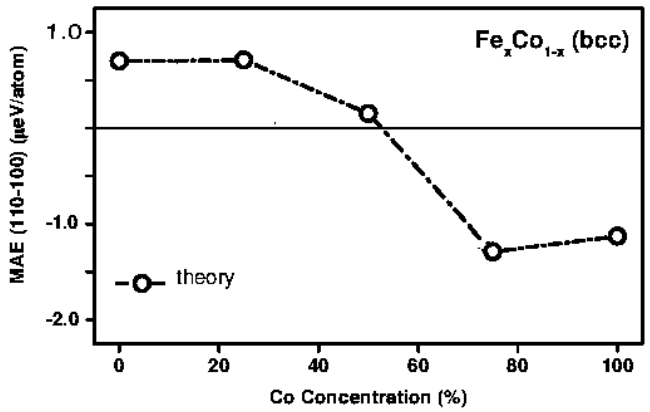

Figure 12. Calculated MAE of the Fe/Co multilayers using the the FP–LMTO method. The calculated points are for bcc Fe, Fe_6Co_2, Fe_4Co_4, Fe_2Co_6 and Co.

approximation. For bcc Fe it was found that a value of ∼1 eV of the Coulomb U reproduced the MAE [42]. However, it was subsequently argued that this value of U differs from the values usually reported [43]. In addition, this value of U also differs from the values used in similar approaches [44] applied to bcc Fe. In addition one may observe that for bcc Fe the observed change in energy, when the magnetization vector (lying in the 110 plane) rotates with an angle θ from the 001 axis, is reproduced within 20% in accurate first principles calculations, based on the local density approximation [45]. These facts, taken together with the data in figure 12, that are at least consistent with the MAE of bulk FeCo alloys, suggest that one does not need to invoke approximations such as the LDA + U for calculations of the MAE of Fe and Co based metallic systems.

5. Conclusions

We discuss in this paper the magnetic and structural parameters of two multilayers, Fe/V and Fe/Co. The electronic structure, magnetic moments (spin and orbital) and Curie temperatures as well as the magneto-crystalline anisotropy are calculated using first principles theory. The calculations were based on a full-potential method, a KKR–ASA method, a non-collinear LMTO–ASA method and a real-space ASA method, and where a comparison can be made the different theories give similar results. Although theory is rather successful in reproducing the experimental data we argue that the observed difference between theory and experiment for the Fe/V multilayers is due to lattice imperfections and that the interface between e.g. Fe and V is not perfectly sharp. Both the magnetic moments as well as the critical temperatures are too large compared to experiment if one assumes perfectly sharp interfaces. A model that involves both the effect of interdiffusion of Fe and V and steps in the interface between the films reproduces the experimental magnetic moments. We also present a model, based on the theory of elasticity, for analysing the structural properties of the Fe/V multilayers. The model reproduces the observed structural parameters of the Fe/V multilayers with rather good accuracy. We have also given a detailed theoretical description of the spin and orbital moments, as well as magneto-crystalline anisotropy of Fe/Co multilayers.

Acknowledgment

Support from the Swedish Natural Research Council (VR) and the foundation for strategic research (SSF) is acknowledged. We also acknowledge support from the Swedish National Supercomputer Facility (NSC). OE is grateful to the Goran Gustafsson foundation for support. Valuable discussions with P Poulopoulos are acknowledged.

References

[1] Sacchi M, Mirone A, Hague C F, Mariot J-M, Pasquali L, Isberg P, Gullikson E M and Underwood J H 1999 *Phys. Rev.* B **60** 12569
[2] Wschwickert M M, Coehoorn R, Tomaz M A, Mayo E, Lederman D, Obrien W L, Lim T and Hare G R 1998 *Phys. Rev.* B **57** 13681
[3] Scherz A, Wende H, Poulopoulos P, Lindner J, Baberschke K, Blomqvist P, Wäppling R, Wilhelm F and Brookses N B 2001 *Phys. Rev.* B **64** 180407
[4] Iseberg P, Hjörvarsson B, Wäppling R, Sundberg E B and Hultman L 1997 *Vacuum* **48** 483
[5] Broddefalk A, Nordblad P, Blomquist P, Isberg P, Wäppling R, Le Bacq O and Eriksson O 2002 In-plane magnetic anisotropy of Fe/V(001) superlattices *J. Magn. Magn. Mater.* **241** 260
[6] Farle M, Anisimov A N, Baberschke K, Langer J and Maletta H 2000 *Europhys. Lett.* **49** 658
[7] Hjörvarsson B, Dura J A, Isberg P, Watanabe T, Udovic T J, Andersson G and Majkrzak C F 1997 *Phys. Rev. Lett.* **79** 901
[8] Liu X, Evans P and Zangari G 2001 *J. Magn. Magn. Mater.* **226–230** 2073
[9] *Landolt–Börnstein New Series* 1984 Group III, vol 19a, ed K H Hellwege and O Madelung (Berlin: Springer)
[10] Bozorth R M 1951 *Ferromagnetism* (New York: Van Nostrand-Reinhold)
[11] Sato N 1990 *J. Appl. Phys.* **67** 4462
[12] Jay J P, Jedryka E, Wojcik M, Dekoster J, Langouche G and Panissod P 1997 *Z. Phys.* B **101** 329
[13] Wojcik M, Jay J P, Panissod P, Jedryka E, Dekoster J and Langouche G 1997 *Z. Phys.* B **103** 5
[14] Söderlind P, Eiksson O, Johansson B, Albers R C and Boring A M 1992 *Phys. Rev.* B **45** 12911
[15] Abrikosov I A, James P, Eriksson O, Söderlind P, Ruban A V, Skriver H L and Johansson B 1996 *Phys. Rev.* B **54** 3380
[16] Turek I, Kudrnovsky J, Drchal V and Weinberger P 1994 *Phys. Rev.* B **49** 3352
[17] Maclaren J M, Schulthess T C, Buttler W H, Sutton R and McHenry M 1999 *J. Appl. Phys.* **85** 4833
[18] Qiu S L, Marcus P M and Morruzzi V K 1999 *J. Appl. Phys.* **85** 4839
[19] Nicklasson A, Johansson B and Skriver H L 1999 *Phys. Rev.* B **59** 6373

[20] Wills J M, Eriksson O and Alouani M 2000 Full-potential LMTO total energy and force calculations *Electronic Structure and Physical Properties of Solids* ed Hugues Dreysse (Berlin: Springer) p 148
[21] Le Bacq O, Johansson B, Eriksson O, James P and Delin A 2002 First principles calculations of the magnetic anisotropy energy of FeV multilayers *Phys. Rev.* B **65** 134430
[22] Andersen O K and Jepsen O 1984 *Phys. Rev. Lett.* **53** 2571
[23] Perdew J P, Burke K and Ernzerhof M 1996 *Phys. Rev. Lett.* **77** 3865
[24] Soven P 1967 *Phys. Rev.* **156** 809
[25] Peduto P R, Frota-Pessoa S and Methfessel M S 1991 *Phys. Rev.* B **44** 13283
Legoas S B *et al* 2000 *Phys. Rev.* B **61** 10417
Frota-Pessoa S, Muniz R B and Kudrnovsky J 2000 *Phys. Rev.* B **62** 5293
[26] Haydock R 1980 *Solid State Physics* vol 35, ed H Ehrenreich, F Seitz and D Turnbull (New York: Academic) p 216
[27] Frota-Pessôa S 1992 *Phys. Rev.* B **46** 14570
[28] Kalska B, Blomquist P, Häggström L and Wäppling R 2001 *J. Magn. Magn. Mater.* **226–230** 1773
[29] Moser A, Krey U, Painter A and Zellermann B 1998 *J. Magn. Magn. Mater.* **151** 341
Moser A, Krey U, Painter A and Zellermann B 1998 *J. Magn. Magn. Mater.* **183** 272
[30] Suss F, Krey U and Krompiewski S 1991 *Acta. Phys. Pol.* A **91** 281
[31] Anisimov A N, Farle M, Poulopoulos P, Baberschke K, Isberg P, Wäppling R, Niklasson A M N and Eriksson O 1999 *Phys. Rev. Lett.* **82** 2390
[32] Uhl M, Sandratskii L M and Kubler J 1994 *Phys. Rev.* B **50** 291
[33] Kubler J 2000 *Theory of Itinerant Electron Magnetism* (Oxford: Oxford University Press)
[34] Skriver H L 1984 *The LMTO Method* (Berlin: Springer)
[35] Sandratskii L M 1998 *Adv. Phys.* **47** 1
[36] Landau D P and Binder K 2000 *A Guide to Monte Carlo Simulations in Statistical Physics* (Cambridge: Cambridge University Press)
[37] Bergqvist L, Nordström L, Svedlindh P and Eriksson O 2002 at press
[38] Mirbt S, Abrikosov I A, Johansson B and Skriver H L 1997 *Phys. Rev.* B **55** 67
[39] Kudrnovsky J, Drchal V, Turek I, Sob M and Weinberger P 1996 *Phys. Rev.* B **53** 5125
[40] Söderlind P, Ahuja R, Eriksson O, Wills J M and Johansson B 1994 *Phys. Rev.* B **50** 5918
[41] Chikazumi S 1997 *Physics of Ferromagnets* (Oxford: Clarendon)
[42] Yang I, Savrasov S Y and Kotliar G 2001 *Phys. Rev. Lett.* **87** 2164051
[43] Stiles M D, Halilov V, Hayman R A and Zangwill A 2001 *Phys. Rev.* B **64** 104430
[44] Lichtenstein A I, Katsnelson M I and Kotliar G 2001 *Phys. Rev. Lett.* **87** 672051
[45] Eriksson O 2001 First principles theory of magnetism of materials with reduced dimensionality *Electonic Structure and Magnetism* ed K Baberschke, M Donath and W Nolting (Berlin: Springer) p 243